

Research on the Clinical Application Possibility of Silicone as a Tissue Filler in Radiotherapy

Wei Li¹, Mei-Fang Fang¹, Lu Xu¹, Lu Cao¹, Wen-Jie Ge¹, Xian-Xiang Wu¹, Han-Fei Cai^{1,*}

¹Department of Radiotherapy, The First Affiliated Hospital of Bengbu Medical College, 233000 Bengbu, Anhui, China

*Correspondence: caihanfeichf@126.com (Han-Fei Cai)

Submitted: 19 September 2022 Revised: 24 November 2022 Accepted: 20 December 2022 Published: 1 June 2024

Background: Due to its good softness, silica gel is now widely used in radiotherapy tissue compensation adhesives, but its relative electron density is high and its CT value is high, so many experts have doubts about its clinical application. This study aimed to explore how silicone can be used as a radiotherapy tissue filler.

Methods: Based on the 6-megavolt (MV) X-ray phase-space file, 30 × 30 × 30 cm cube models of water, silicone, and different human tissues were constructed in Geant4 Monte Carlo (MC) software to simulate the transport process of X-rays in those media. The study obtained the central axial energy deposition in silicone and the particle-phase-space information at a depth of 1 cm and 2 cm when the rays passed through all the media.

Results: The radiation attenuation in silicone was greater than in water. At a depth of 5 cm, the thickness of the silicone was equivalent to 1.12 times the thickness of the water. In dose built-up area and approximate charged-particle equilibrium, the particle-phase-space composition in silicone were similar to that in water, skin, soft tissue, and adipose tissue, although the particle-phase-space concentration of positrons was slightly higher, and the energy spectrum of each particle was distributed more uniformly. The particle-phase-space composition in silicone was quite different from that in compact bone and cortical bone, and the particle-phase-space concentration of positrons was lower in silicone than in the two bones media. The MC and Pinnacle algorithms were in good agreement in terms of the dose calculation behind the silicone. After the rays had passed through the different thicknesses of silicone, the differences in the two algorithms were within 2.5%.

Conclusion: There was negligible impact of secondary dose build-up between the silicone and the body's surface, and the values calculated by the different treatment planning system (TPS) algorithms were in good agreement. Therefore, silicone is deemed suitable for use as a tissue filler from the perspective of dosage.

Keywords: silicone; tissue filler; energy spectrum; phase-space information; Monte Carlo; treatment planning system

Introduction

To overcome the build-up effect of the megavolt-level X-ray doses generated by radiotherapy accelerators, often, when treating superficial tumors, tissue filler is added to the corresponding positions on the body's surface. Tissue filler has a certain hardness, and the surface of the human body is often uneven; therefore, operations (e.g., surgery) can result in scars and other protrusions on the body's surface, forming cavities between the filler and the skin. These cavities affect the body surface dose [1–6], and due to the limitations of the treatment planning system (TPS) in dealing with heterogeneous tissue, errors can occur, even when filler is added during positioning and these cavities are considered during dose calculation [7–10]. However, there is no guarantee that the cavities created by each positioning will be the same across all localizations. Therefore, to ensure the conformability and applicability of filler to the body's surface, three-dimensional (3D) printing or softer materials are used. As silicone is softer than previous commercial fillers, it is a popular choice for 3D printing [11], although even

conventional fillers can be made of silicone [12]. Due to the comparatively low cost of silicone fillers, patients may even choose to purchase these themselves, thereby avoiding cross-infection risks from the sharing of fillers among patients. Nevertheless, the electron density of silicone is high, and further research is needed to explore its suitability for use as a tissue filler.

The Monte Carlo (MC) algorithm is the gold standard for radiation dose calculation and is widely used in radiotherapy [5,6,8–10,13,14]. Geant4 is a set of open-source MC software packages [15] with an increasingly important role in many fields, including particle physics, nuclear physics, and medical physics. The Monaco TPS (developed by Elekta) is widely favored in the field of oncology radiotherapy, where the MC algorithm is traditionally used for dose calculation. The X-ray voxel Monte Carlo (XVMC) ROM algorithm calculation accuracy close to receive card [16] is radiation dose in the calculation of a classical algorithm, with the development of radiation therapy for many years of application, widely used in clinic, convolution iteration (CC) algorithm is radiation dose calcula-

Table 1. Densities, relative electron densities and effective atomic numbers of different materials.

Medium	Mass density (g/cm ³)	Electron density (electron number/cm ³ /10 ²³)	Effective atomic number
Water	1.000	3.346	7.428
Skin	1.090	3.609	7.276
Soft tissue	1.030	3.426	7.219
Fat	0.950	3.186	6.343
Compact bone	1.850	5.914	11.689
Cortex of bone	1.920	5.958	13.299
Silica gel	1.155	3.760	10.409

tion in another classic algorithm, with the development of radiation also have applied for many years. Pinnacle plan system is a plan design software developed by Philips in the Netherlands. Its hyperposition folded cone convolution (CCCS) algorithm has been widely used in clinical treatment for many years, and its algorithm reliability has been widely recognized. The present study used Geant4 to investigate the phase-space information of 6-megavolt (MV) X-ray passing through silicone, water, and various human tissues after reaching approximate charged-particle equilibrium (2 cm). It explored the possibility of using silicone as a radiotherapy tissue filler by comparing the results from different Monaco TPS and Pinnacle algorithms that were used to calculate solid water surface doses after radiation had passed through silicone.

Materials and Methods

Materials

This study used Geant4 (version 10.02.p02, European Organization for Nuclear Research, Meyrin, Switzerland) software with a 64-bit Windows 7 operating system (Microsoft, Redmond, WA, USA). The C++ compiler was Visual Studio 2013 (Microsoft, Redmond, WA, USA), and the physical model was G4EmPenelopePhysics (cut-off range: 0.1 cm). Other materials included the Monaco TPS (version 5.1, Elekta, Stockholm, Sweden), Pinnacle Treatment Planning System (version 9.1, Philips, Amsterdam, Holland), a general-purpose large-aperture computerized tomography scanner, a silicone membrane, and solid water. Data processing and plotting were conducted using Origin-Pro 2018C (64-bit) (OriginLab, Northampton, MA, USA) software.

Construction of Phantoms of Different Media

Different media, including water, skin, soft tissue, adipose tissue, compact bone, cortical bone, and silicone, were constructed in the Geant4 MC package with water and each human tissue using the available media, respectively [17], as follows: G4_WATER, G4_SKIN_ICRP, G4_TISSUE_SOFT_ICRP, G4_ADIP

OSE_TISSUE_ICRP, G4_BONE_COMPACT_ICRU, and G4_BONE_CORTICAL_ICRP. The silicone (Oulaite Medical Technology (Wuxi) Co., Ltd., Wuxi, China) comprised the following constituent elements: silicon (37.84%), carbon (32.43%), oxygen (21.62%), and hydrogen (8.11%). The density of each medium, the calculated electron density, and the effective atomic serial number for each medium according to the corresponding equation are listed in Table 1 [17]. A 30 × 30 × 30 cm cube with the upper surface located at the level of the source axis of the accelerator (i.e., 100 cm) was constructed using each of the different media sequentially. A small voxel was constructed on the central axis of the incident rays in the cube to record the dose deposition, and a 16 × 16 cm voxel with a thickness of 0.1 cm perpendicular to the direction of the incident radiation was constructed at a depth of 1 cm and 2 cm, respectively, in the phantom to record the phase-space information of the rays at the site.

Acquisition of Particle-Phase-Space Information in Different Materials

The phase-space file obtained by the head model of an Elekta Infinity accelerator with a tungsten gate of 10 × 10 cm was used as the particle source file [10]. The rays were stimulated sequentially to pass through the phantoms of the different media described in section 1.2 to obtain the radiation dose deposition on the central axis in each phantom and particle-phase-space file at a depth of 1 cm and 2 cm. The total particle number, particle average energy, photon number, photon average energy, electron number, electron average energy, positron number, and positron average energy in each phase-space file were read and recorded by programming, and an energy interval of 0.05 MeV was used to record the photon number, electron number, and positron number in each energy range.

Calculation of the Solid Water Surface Dose Behind Silicone by the Treatment Planning System

A 30 × 30 × 30 cm cube phantom was constructed on the Monaco TPS and Pinnacle, and bolus thicknesses of 0.3, 0.5, and 1.0 cm were outlined on its surface. The center of the contact surface between the bolus and solid water was set as the isocenter and reference point in the TPS, and a 10 × 10 cm field with gantry and secondary collimator angles of 0° was established. X-ray voxel Monte Carlo (XVMC) algorithm in Monaco, convolution iteration algorithm and superposition folded cone convolution algorithm (CCCS) in Pinnacle were used to calculate the dose distribution of 100 MU under different thickness silica gel, and the reference point dose was recorded.

Data Processing

In the present study, particle relative intensity (PRI) (in Eqn. 1 below) was used to describe the energy spectrum distribution of the particles. The data in the phase-space file

Table 2. Comparison of particles phase-space in different mediums in 1 cm depth.

	Water	Skin	Soft tissue	Fat	Compact bone	Cortex of bone	Silica gel
Photon percentage (%)	73.45 ± 0.12	72.68 ± 0.12	73.22 ± 0.12	74.17 ± 0.13	67.23 ± 0.11	66.88 ± 0.11	71.74 ± 0.12
Photon energy (Mev)	1.513 ± 0.003	1.500 ± 0.003	1.509 ± 0.003	1.520 ± 0.003	1.434 ± 0.002	1.441 ± 0.002	1.504 ± 0.003
Electron percentage (%)	26.26 ± 0.07	27.03 ± 0.07	26.51 ± 0.07	25.59 ± 0.07	32.30 ± 0.08	32.56 ± 0.08	27.88 ± 0.08
Electron energy (Mev)	0.5323 ± 0.0015	0.5370 ± 0.0015	0.5344 ± 0.0015	0.5300 ± 0.0015	0.5650 ± 0.0014	0.5618 ± 0.0013	0.5337 ± 0.0015
Positron percentage (%)	0.2900 ± 0.0079	0.2872 ± 0.0077	0.2726 ± 0.0075	0.2409 ± 0.0072	0.4612 ± 0.0093	0.5549 ± 0.0102	0.3812 ± 0.0089
Positron-decay energy (Mev)	0.7124 ± 0.0193	0.7219 ± 0.0194	0.7234 ± 0.0201	0.7163 ± 0.0214	0.7507 ± 0.0151	0.7454 ± 0.0136	0.7135 ± 0.0166

Table 3. Comparison of particles phase-space in different mediums in 2 cm depth.

	Water	Skin	Soft tissue	Fat	Compact bone	Cortex of bone	Silica gel
Photon percentage (%)	72.91 ± 0.11	72.25 ± 0.11	72.66 ± 0.11	73.38 ± 0.11	67.40 ± 0.10	67.01 ± 0.10	71.40 ± 0.11
Photon energy (Mev)	1.488 ± 0.002	1.471 ± 0.002	1.483 ± 0.002	1.496 ± 0.002	1.390 ± 0.002	1.399 ± 0.002	1.477 ± 0.002
Electron percentage (%)	26.80 ± 0.07	27.47 ± 0.07	27.07 ± 0.07	26.38 ± 0.07	32.15 ± 0.07	32.45 ± 0.07	28.22 ± 0.07
Electron energy (Mev)	0.5318 ± 0.0014	0.5359 ± 0.0013	0.5322 ± 0.0014	0.5311 ± 0.0014	0.5557 ± 0.0012	0.5514 ± 0.0012	0.5304 ± 0.0013
Positron percentage (%)	0.2831 ± 0.0071	0.2809 ± 0.0070	0.2712 ± 0.0069	0.2335 ± 0.0065	0.4497 ± 0.0084	0.5440 ± 0.0093	0.3776 ± 0.0081
Positron-decay energy (Mev)	0.7122 ± 0.0178	0.7196 ± 0.0179	0.7156 ± 0.0182	0.7185 ± 0.0199	0.7488 ± 0.0141	0.7498 ± 0.0128	0.7101 ± 0.0152

was input to the Origin 2018 64-bit (OriginLab, Northampton, MA, USA) software for statistical analysis and plotting.

$$PRI = \frac{N_{P,E}}{N_P} \times 100\% \quad (1)$$

In Eqn. 1, $N_{P,E}$ represents the number of particles of type P in the 0.05-MeV energy grid centered on E, and N_P represents the total number of particles of type P.

The difference in the dose of different algorithms for treatment planning systems (D in Eqn. 2 below) of the solid water surface after rays had passed through different thicknesses of silicone (calculated by the MC and CC algorithms) is shown in Eqn. 2:

$$D = \frac{D_{MC} - D_{CC}}{D_{CC}} \times 100\% \quad (2)$$

where D_{MC} represents the solid water surface dose calculated by the Monaco MC algorithm, and D_{CC} represents the solid water surface dose calculated by other algorithms.

Results

Central Axis Dose Deposition

The dose depositions of rays in water and silicone on the central axis of the rays are shown in Fig. 1. At approximately 1.55 cm (which was taken as the reference dose), the maximum dose depths were very similar. Therefore, it could be inferred that in the dose build-up region, the dose in silicone was higher than in water. Radiation behind the dose build-up region was attenuated faster in silicone; thus, the dose in silicone was lower than in water at the same depth. However, after the silicone depth was multiplied by a coefficient of 1.12, the dose variations in water and silicone were highly consistent up to a depth of 5 cm.

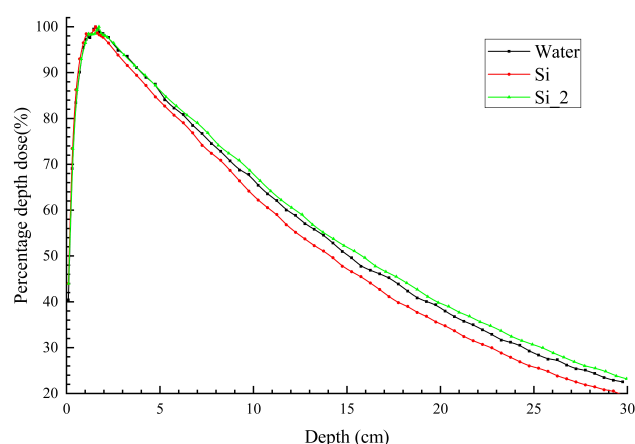


Fig. 1. Percentage depth dose curves of 6-megavolt (MV) X-ray among water and silica-gel. Water describes the curve in water; Si describes the curve in silica-gel; Si_2 describes the curve in silica-gel with the depth multiplied by 1.12.

Comparison of Basic Particle Information

Tables 2,3 present comparisons of the particle-phase-space information of 6-MV X-ray at a depth of 1 cm and 2 cm in different media. Considering the differences in the attenuation coefficients in different media, the particle ratio is expressed as the percentage of the total number of particles in each medium comprising particles of interest in that medium. It is evident that whether it's in the dose-built zone or the near-charged particle equilibrium zone, while both the percentages and average energies of photons and electrons in silicone were similar to those in water, skin, soft tissue, and adipose tissue, the percentage of positrons in silicone was slightly higher than in each of those four media. There were significant differences in the percentages of particles and average energies between silicone and the above four media and between silicone and compact/cortical bone. The percentages of positrons in silicone and water, skin, soft tissue, and adipose tissue were significantly lower than those in compact bone and cortical bone.

Comparison of Energy Spectra

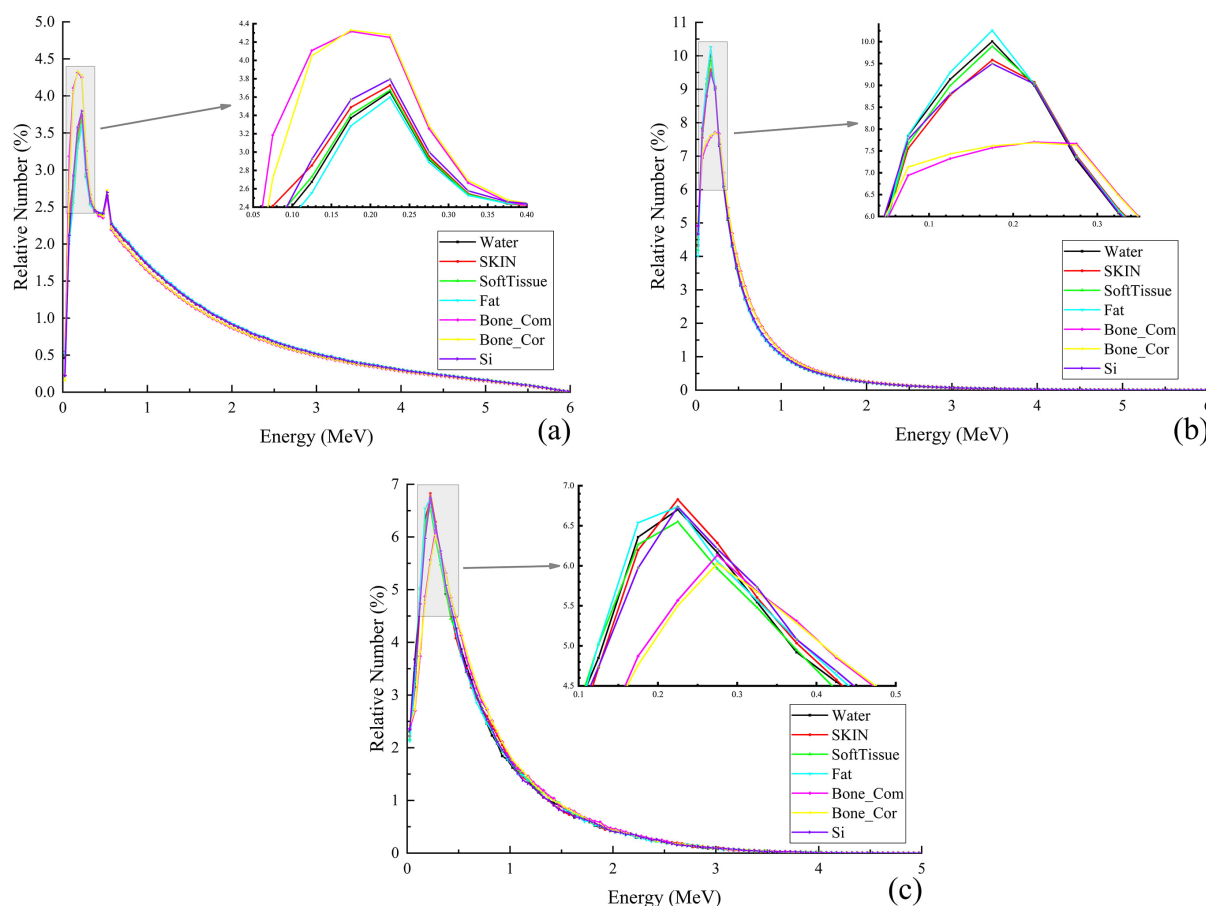
The energy spectra of photons, electrons, and positrons at a depth of 2 cm in different media are shown in Fig. 2. This data suggests that the particle energy spectra in water, skin, soft tissue, adipose tissue, and silicone were relatively consistent, while those in compact bone and cortical bone were close to each other but differed from those in the other five media. The low-energy part of the photon energy spectrum formed a slightly higher proportion in silicone than in water, skin, soft tissue, and adipose tissue, but the proportion was much lower than in compact bone and cortical bone. At increased energies, the photon energy spectrum in silicone became roughly the same as the spectra in water, skin, soft tissue, and adipose tissue, but it was larger than those in compact and cortical bone. In terms of the electron energy spectrum, the percentage of low-energy parts was slightly lower in silicone than in water, skin, soft tissue, and adipose tissue, although it was higher than in compact and cortical bone (maximum difference of approximately 1.6%). With an increase in energy, the energy spectra in silicone and the two bones media converged. The positron energy spectra in compact bone and cortical bone were similar to the electron energy spectra (Fig. 3).

Comparison of the Solid Water Surface Dose Calculated by Different Algorithms

Table 4 shows the calculated surface dose values of solid water in the center of the field under different thickness of silica gel by Monte Carlo and convolution iterative algorithms and Pinnacle treatment planning system superposition folded cone convolution algorithm, respectively, in Monaco treatment planning system. The differences between the solid water surface doses calculated at different silicone thicknesses using the two algorithms were relatively small (maximum difference of 2.3%). For the range

Table 4. Comparison of the solid water surface dose calculated with different algorithms when the X-ray pass through silica gel.

Thickness of the silica gel (cm)	X-ray voxel Monte Carlo algorithm to calculate the values (Gy)	Convolution iterative algorithm computes the values (Gy)	Value calculated by super-position folded cone convolution algorithm (Gy)	Difference (%)
0.3	0.795	0.789	0.792	0.760
0.5	0.896	0.880	0.886	1.818
1.0	1.023	1.000	1.014	2.300


Fig. 2. Energy spectrum distributions of particles in different mediums at 1 cm. (a) is photon energy spectrum. (b) is electron energy spectrum. (c) is positron energy spectrum.

of thicknesses of tissue filler used in clinical practice, the differences between the surface doses calculated by the two algorithms were small, and the dose allowance for clinical practice was not exceeded with either algorithm.

Discussion

Radiation therapy has entered the era of three-dimensional precision, involving precise positioning, planning, and treatment; however, the fact that the cavity under a tissue filler affects the precision of radiotherapy for superficial tumors overshadows the potential of this technique [14]. Previously, in addition to conformability and softness, tissue equivalence was an important factor in the selection of filler materials [15]. In recent years, with the advancement of radiotherapy TPS algorithms and treatment tech-

nology, dose calculation is more accurate in heterogeneous tissues, researchers have begun using new materials [16]. Among these, silicone, with its softness and conformability, has become the most widely used materials [17]. However, there is little research on whether this material can meet the tissue equivalence specifications required for radiotherapy.

The present study investigated the energy deposition patterns and particle-phase-space information in silicone and compared them with those in water and several types of human tissues. The results revealed that the attenuation of radiation in silicone was greater than in water, and the relationship of 1:1.12 was basically satisfied within the required thickness of the tissue filler, i.e., silicone with a thickness of 1 cm was equivalent to the build-up effect of water with a thickness of 1.12 cm. The consistency found in the max-

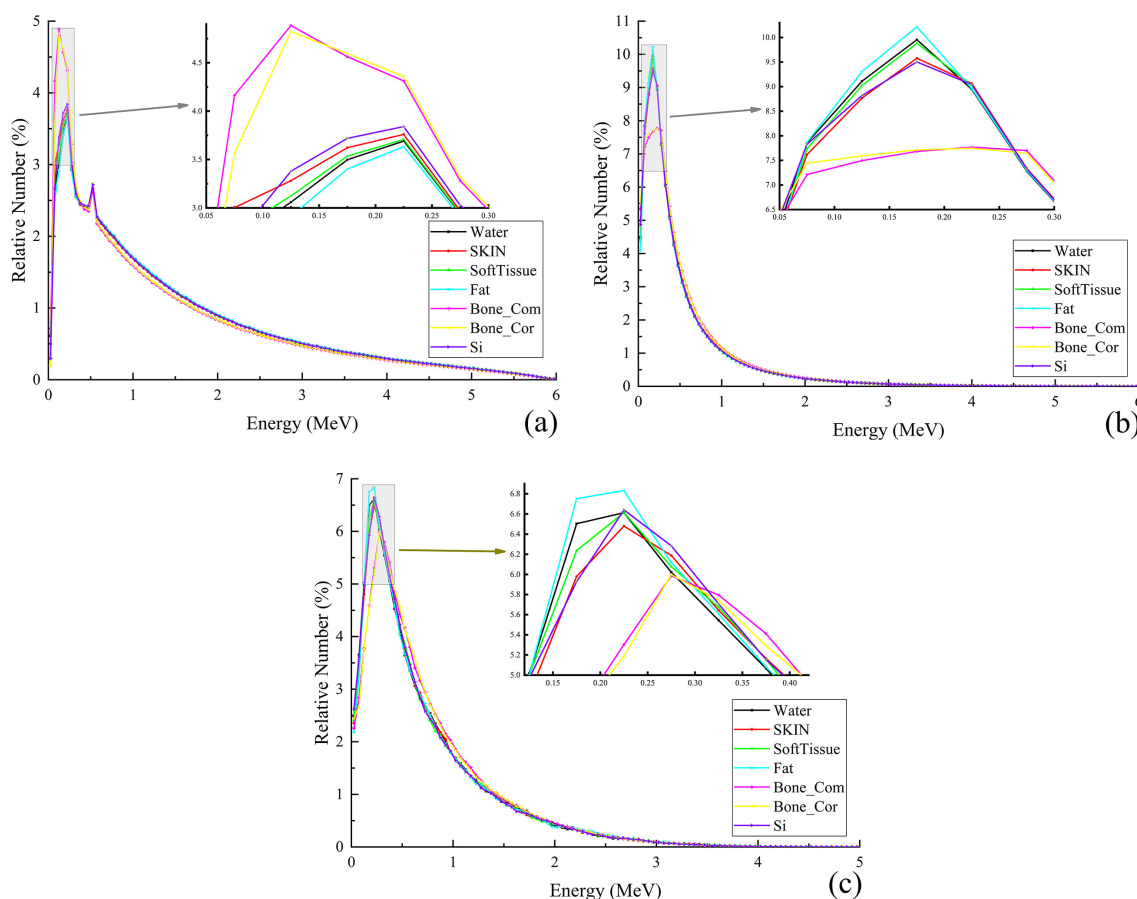


Fig. 3. Energy spectrum distributions of particles in different mediums. (a) is photon energy spectrum. (b) is electron energy spectrum. (c) is positron energy spectrum at 2 cm.

imum dose depth between silicone and water might be due to a calculation error. In both of 1 cm depth dose proper place and the depth of 2 cm of charged ions approximate balance, silica gel in the photon, electron proportion and average energy and water, skin and soft tissue, fat, but differ with compact bone and bone cortex is bigger, positron proportion between the skin and bone, it may be associated with silicon content is higher in silica gel; the energy spectrum distribution of the three kinds of particles in silica gel is between the human tissue, which is very close to the skin, and even closer to the skin than water in the electron spectrum distribution. Therefore, the secondary dose-building effect caused by silica gel as tissue filler in the skin will be very small. In the range of tissue filling thickness commonly used in clinical practice, the difference of solid water surface dose after silica gel calculated by X-ray voxel Monte Carlo algorithm, convolutional iterative algorithm and Pinnacle in Monaco was less than 2.5%, which met the clinical needs. The results indicate that there is little difference between the epidermal dose calculated by different treatment planning systems and different algorithms when silica gel is used as tissue filler material, which proves that the use of silica gel as tissue filler will not cause a large error in the calculation of surface dose.

Based on the Monte Carlo algorithm, this study compared the differences in ray attenuation and particle phase spatial information distribution between silica gel, water and human tissue in the dose-built area and approximate charged particle equilibrium area, and compared the surface dose of solid water calculated by different algorithms of different treatment planning systems after the radiation passed through different thickness of silica gel. Although these comparisons suggest that silicone is a promising tissue filler material, further studies are needed to determine whether other algorithms or other versions of treatment planning systems can ensure the accuracy of tissue dosage under silicone. This study sheet is studied from the aspects of physical dosimetry silica gel applied to the clinical possibility, to truly applied to clinical, still need to by measuring compared with the data treatment planning system, to further ensure the silicone material filler not cause treatment planning system to calculate tissue surface dose of bigger error, at the same time when applications need to carefully observe the patient's response to treatment, to determine whether it can be applied to the clinic. Better flexibility based on silica gel materials, can with the patient skin more relevant, reduces with the skin, the cavity between the patients, in turn, increases the surface dose, at the same time due to the current

commercial organization filler much cheaper price, without significantly increased under the condition of economic burden for patients of personnel is special, is helpful to reduce the patient to hospital infection, However, if silica gel is used as tissue filler, there will be relatively high positron production. Whether this will lead to an increase in the dose to normal tissues in the field remains to be further demonstrated.

Conclusion

There was negligible impact of secondary dose build up between the silicone and the body's surface, and the values calculated by the different TPS algorithms were in good agreement. Therefore, silicone is deemed suitable for use as a tissue filler from the perspective of dosage.

Availability of Data and Materials

The datasets used and/or analysed during the current study available from the corresponding author on reasonable request.

Author Contributions

WL and HFC designed the research study; WL, MFF, LX, LC, WJG, XXW and HFC performed the research; WL, MFF, LX, LC, WJG, XXW and HFC collected and analyzed the data. WL and HFC has been involved in drafting the manuscript. All authors have been involved in revising it critically for important intellectual content. All authors gave final approval of the version to be published. All authors have participated sufficiently in the work to take public responsibility for appropriate portions of the content and agreed to be accountable for all aspects of the work in ensuring that questions related to its accuracy or integrity.

Ethics Approval and Consent to Participate

Not applicable.

Acknowledgment

Not applicable.

Funding

This research received no external funding.

Conflict of Interest

The authors declare no conflict of interest.

References

- [1] Khan Y, Villarreal-Barajas JE, Udowicz M, Sinha R, Muhammad W, Abbasi AN, *et al.* Clinical and Dosimetric Implications of Air Gaps between Bolus and Skin Surface during Radiation Therapy. *Journal of Cancer Therapy*. 2013; 4: 1251–1255.
- [2] Butson MJ, Cheung T, Yu P, Metcalfe P. Effects on skin dose from unwanted air gaps under bolus in photon beam radiotherapy. *Radiation Measurement*. 2000; 32: 201–204.
- [3] Chung JB, Kim JS, Kim IA, Lee JW. Surface Dose Measurements from Air Gaps under a Bolus by Using a MOSFET Dosimeter in Clinical Oblique Photon Beams. *Journal of the Korean Physical Society*. 2012; 61: 1143–1147.
- [4] Wang YF, Dona O, Liu K, Adamovics J, Wu CS. Dosimetric characterization of a body-conforming radiochromic sheet. *Journal of Applied Clinical Medical Physics*. 2020; 21: 167–177.
- [5] Kong D, Hui L, Wei XD, Kong Y, Ding Y, Kong X, *et al.* Effect of submembrane cavity space on superficial tissue dose. *Chinese Journal of Radiation Oncology*. 2018; 27: 1009–1013.
- [6] Kong D, Hui L, Wei XD, Kong Y, Ding Y, Kong X, *et al.* Effect of Bolus and skin cavity on dose deposition in shallow tissue. *Chinese Journal of Radiation Oncology*. 2019; 28: 27–31.
- [7] Codel G, Serin E, Pacaci P, Sanli E, Cebe M, Mabhouti H, *et al.* SU-F-SPS-01: accuracy of the small field dosimetry using acuros XB and AAA dose calculation algorithms of eclipse treatment planning system within and beyond heterogeneous media for truebeam 2.0 unit. *Medical Physics*. 2016; 43: 3350.
- [8] Ramachandran P, Smith A, Hagekyriakou J, Hughes J, Lonski P, Howard B, *et al.* Contralateral breast dose with electronic compensators and conventional tangential fields - A clinical dosimetric study. *Zeitschrift Fur Medizinische Physik*. 2021; 31: 347–354.
- [9] Kong D, Kong XD, Hui L, Wei XD, Zhao YT, Yang B. Effect of compensated submembrane cavity on calculation of shallow dose in radiotherapy planning system. *Cancer Prevention and Treatment*. 2021; 34: 64–69.
- [10] Hou YJ, Yu JP, Wang YQ, Liu HR, Li D, Xu JJ, *et al.* Preparation and preclinical study of 3D printed silica gel BOLus for chest wall. *Chinese Journal of Radiation Oncology*. 2018; 27: 835–838.
- [11] Aisyah S, Carina CCC, Nazara T, Sekartaji G, Nainggolan A. A Comparative Study of Dosimetric Characterization of Bolus Based on Natural Rubber (*Hevea Brasiliensis*) and Clinical Bolus for Therapy with Megavolt Electron Radiation. *Journal of Physics Conference Series*. 2020; 1505: 012026.
- [12] Arbor N, Gasteuil J, Noblet C, Moreau M, Meyer P. A GATE/Geant4 Monte Carlo toolkit for surface dose calculation in VMAT breast cancer radiotherapy. *Physica Medica*. 2019; 61: 112–117.
- [13] Wang L, Ding GX. The accuracy of the out-of-field dose calculations using a model based algorithm in a commercial treatment planning system. *Physics in Medicine and Biology*. 2014; 59: N113–N128.
- [14] Geant4 Collaboration. Introduction to Geant4 [EB/DL]. Available at: <https://geant4-userdoc.web.cern.ch/UsersGuides/IntroductionToGeant4/html/index.html> (Accessed: 18 July 2017).
- [15] Al Halabi H, Hou Z, Schantz PN, Shakibnia L, Swanson JW, Cavanaugh SX. Repeat Courses of Stereotactic Radiation Therapy for Treatment of Patients With Brain Metastases—Dosimetric Implications and Risk of Radiation Necrosis. *International Journal of Radiation Oncology, Biology, Physics*. 2020; 108: e323.
- [16] Geant4 Collaboration. User's Guide: For Application Developers [EB/DL]. Available at: <https://geant4-userdoc.web.cern.ch/UsersGuides/ForApplicationDeveloper/BackupVersions/V10.2/html/apas06.html> (Accessed: 18 July 2017).
- [17] Hu YM, Zhang HZ, Dai JR. *Radiation Oncology Physics*. Atomic Energy Press: Beijing. 1999.